Tailoring the Spin Functionality of a Hybrid Metal-Organic Interface by Means of Alkali-Metal Doping

Mirko Cinchetti,* Sabine Neuschwander, Alexander Fischer, Andreas Ruffing, Stefan Mathias, Jan-Peter Wüstenberg, and Martin Aeschlimann

Department of Physics and Research Center OPTIMAS, University of Kaiserslautern, 67663 Kaiserslautern, Germany

(Received 15 January 2010; published 25 May 2010)

We employ a recently developed purpose-made technique based on spin-resolved two-photon photoemission spectroscopy to study the influence of alkali-metal doping (Cs and Na) on the spin functionality of the interface between a cobalt thin film and the organic semiconductor copper phthalocyanine. We find two alkali-metal-induced effects. First, alkali-metal atoms act as impurities and increase the spin-flip probability for the electrons crossing the interface (detrimental effect). Second, they allow one to modify the interface energy level alignment and, consequently, to enhance the efficiency of spin injection at an arbitrary energy above the Fermi level of the cobalt (intrinsic effect). We show that the intrinsic effect dominates over the detrimental one, opening the possibility to actively tailor the spin functionality of the considered hybrid metal-organic interface by changing the doping concentration.

DOI: 10.1103/PhysRevLett.104.217602 PACS numbers: 79.60.Fr, 72.25.Mk, 75.70.Cn, 81.05.Fb

Organic semiconductors (OSC) have demonstrated their potential as a new class of materials for a variety of versatile and very-low-cost electronic devices based on organic thin films [1], such as organic light emitting diodes (OLEDs), organic thin-film transistors, and organic photovoltaic cells. As for the case of inorganic-semiconductor-based electronics, doping constitutes a very valuable pathway to systematically tune the electronic properties of OSC and thus their performance in devices [2–5]. For example, doping of OLEDs is one of the most effective methods to control the luminescence of the emitter [3] and to enhance the device stability [4] as well as the charge injection [5].

A new class of possible applications for OSC opened up with the discovery of magnetoresistive effects in spin-valve configurations consisting of metallic ferromagnetic electrodes spaced by an organic layer [6,7]. Starting from those pioneering experiments, significant efforts have been made to integrate OSC in the field of spintronics [8]. The two fundamental requirements for engineering organic spintronics devices are (i) the efficient injection of spin-polarized carriers at a hybrid inorganic-organic interface (where the inorganic material acts as a source of spin-polarized carriers), and (ii) a suitable spin diffusion length in the OSC itself. Recent experiments with specifically designed experimental techniques, low-energy muon rotation [9], and spin-resolved two-photon photoemission spectroscopy (SR-2PPE) [10] have proven the feasibility of high efficiency spin injection into OSC [10] and reported spin diffusion lengths on the order of some tens of nanometers [9,10]. Thus, no fundamental obstacle thwarts the development of organic spintronics devices. Since OSC are generally characterized by moderate spin diffusion lengths but very long spin lifetimes [11], the most straightforward and promising route for application of OSC in spintronics is to exploit the high spin-injection efficiency achievable in OSC [12]. In this context, the ability to control and tune the spin functionality of hybrid metal-organic interfaces is a central issue.

In this Letter, we devote ourselves to this topic and provide the proof of principle that doping of OSC allows one to systematically tune the spin properties of a hybrid ferromagnetic metal-OSC interface. To do so, we employ the SR-2PPE technique, allowing one to quantify the spin properties of the considered interface in terms of a set of microscopic parameters that fully characterize its spin functionality in the accessible energy range, the so-called [10] pure spin-injection region (PSI).

The experiments were performed on the interface between a cobalt thin film and the OSC copper phthalocyanine (CuPc). Cobalt films of 3.5 nm thickness were grown by electron beam epitaxy on a Cu(001) crystal, resulting in a metastable, tetragonally distorted, face-centered cubic structure with in-plane uniaxial magnetic anisotropy along the [110] direction of the Cu substrate. CuPc thin films with thickness of 0.68 nm (corresponding to 2 monolayers) were deposited *in situ* on the freshly prepared Co film at a rate of 0.01 $\mathrm{nm\,s^{-1}}$. *In situ* sample deposition enables preparation of well-defined high-quality interfaces; more details on the growth of the Co-CuPc system can be found in [10,13]. As dopants for CuPc, we have chosen the alkali metals cesium and sodium, evaporated from two SAES Getters sources. The choice of Cs and Na was conditioned, on the one hand, by the fact that the effects of alkali-metal doping on the electronic structure of both the occupied and unoccupied states of CuPc has been studied in detail in the literature [14–16], and on the other hand, by the fact that alkali-metal atoms are known to readily diffuse into CuPc [17], so that a uniform alkali-metal concentration can be assumed in the deposited CuPc films.

The experimental setup used for the SR-2PPE experiments is similar to that reported in [10,18]. In brief, a

Ti:sapphire laser is used as a pulsed light source. The system delivers sech^2 temporal shaped pulses of up to 10 nJ/pulse with a duration of 18 fs at a repetition rate of 76 MHz and a wavelength of 790 nm. The linearly polarized laser output is frequency doubled in a 0.2 mm thick barium-borate crystal to produce UV pulses at photon energy $h\nu = 3.1$ eV. The angle of incidence of the laser beam on the sample is 45°; the fluence is 6 $\mu\mathrm{J\,cm^{-2}}$. The photoemitted electrons are analyzed in normal emission geometry in an ultrahigh vacuum system equipped with a commercial cylindrical sector energy analyzer (Focus CSA 300) and a spin detector based on spin-polarized low-energy electron diffraction (Focus SPLEED). Ultraviolet photoelectron spectroscopy (UPS) has been performed using a commercial vacuum UV source (Focus, model HIS 13) driven at 21.22 eV (He Ia line) and a 45° angle of incidence to the sample. The photoelectrons were collected at normal emission using a hemispherical energy analyzer for parallel energy and momentum detection (SPECS Phoibos 150) set to $\Delta E = 20$ meV and $\Delta q = 0.15°$.

In order to understand the spin-resolved data it is essential to determine the effect of doping on the energy level alignment at the Co-CuPc interface. Figure 1 shows the UPS spectra recorded from 0.68 nm CuPc on cobalt under progressive Na doping as a function of the energy $E - E_F$, with E_F being the Fermi energy of the cobalt. The left panel shows the low-energy cutoff, reflecting the position of the vacuum level and thus of the work function of the sample, while the right panel depicts the region of the highest occupied molecular orbital (HOMO) of CuPc. In the spectra, the energetic positions of the low-energy cutoff and of the HOMO onset are marked, respectively, with green diamonds and blue circles. Clearly, doping with Na atoms induces a shift of both the low-energy cutoff and of the HOMO onset to lower energies. The almost identical dependency of both shifts on the Na exposure time is plotted in the lower panel of Fig. 1. A very similar behavior was observed for Cs doping (not shown). Our results are in line with the data reported in [14–16] for thicker (10–15 nm) CuPc films on Au, where the shift of the energy levels has been attributed to charge transfer from the alkali metals to CuPc. In line with this interpretation, if we assume the observed shifts to be only slightly substrate dependent, we can use the shifts vs doping ratio curves measured in [15,16] by x-ray photoemission spectroscopy to obtain a rough estimate of the alkali-metal atom to CuPc molecule ratio (R_{Na}, R_{Cs}) in our samples. In the measurements presented in the following, the doping time was set to obtain a HOMO shift of (0.50 ± 0.05) eV, corresponding to $R_{\mathrm{Na}} \approx 1.7$ and $R_{\mathrm{Cs}} \approx 0.2$. Compared to Na, less Cs atoms are required to obtain a comparable shift as a consequence of the lower ionization energy of Cs [15]. At the doping ratios used for both Na and Cs, the electronic structure of CuPc is preserved and inverse photoemission (IPES) studies have shown that the lowest unoccupied molecular orbital (LUMO) shifts identically to the HOMO, so that the band gap of CuPc remains constant while the Fermi level shifts within the energy gap [15]. Accordingly, higher lying CuPc molecular orbitals (MOs) are shifted energetically within the PSI, while the PSI itself is extended by 0.5 eV [19], as schematically shown in Fig. 2.

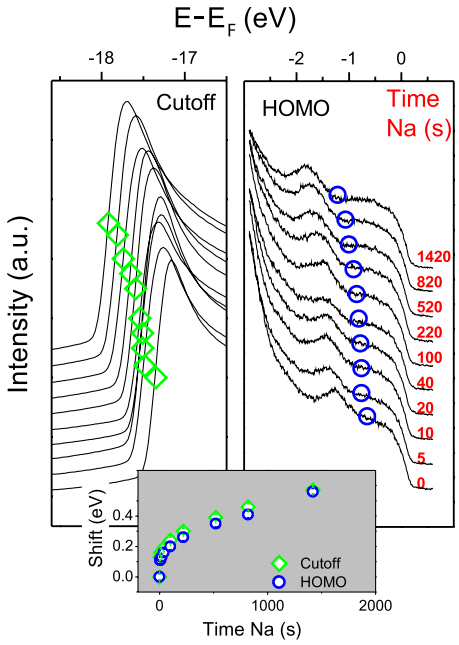

FIG. 1 (color online). UPS spectra recorded from 0.68 nm CuPc on cobalt for different Na exposition times. Left panel: low-energy region of the spectrum, with cutoff position marked with green diamonds. Right panel: HOMO region of CuPc, with HOMO onset marked with blue circles. Lower panel: shift of the low-energy cutoff and of the HOMO onset positions as a function of Na exposition time, extracted from the UPS spectra.

In order to study the spin properties of the Co-CuPc, Co-CuPc:$\mathrm{Cs}_{0.2}$, and Co-CuPc:$\mathrm{Na}_{1.7}$ interfaces, shortly denoted as Co-CuPc:A (with A = Cs, Na, or ∅ for no doping), we employed SR-2PPE. Figure 2 shows the conceptual principle of the experiments: spin-polarized electrons are excited in the cobalt substrate by a first photon ($h\nu = 3.1$ eV) into unoccupied states with energy E^* below the vacuum level E_{vac}. E^* is the injection energy, defined as the excess energy of the excited electrons referenced to E_F. The excited (hot) electrons move in all directions out of the excitation volume. A fraction of them will eventually reach the Co-CuPc:A interface, i.e., be *injected* from Co into CuPc:A, where photoemission can take place if a second photon (not shown in Fig. 2) is absorbed within the temporal width of the laser pulse (27 fs). More precisely, the intermediate state of the two-photon photoemission will be a molecule-metal hybrid state, with degree of hybridization depending on the coupling strength between cobalt and CuPc:A. Thus, when referring to spin injection into CuPc:A in the following, we will mean injection into such a hybrid state. Note that

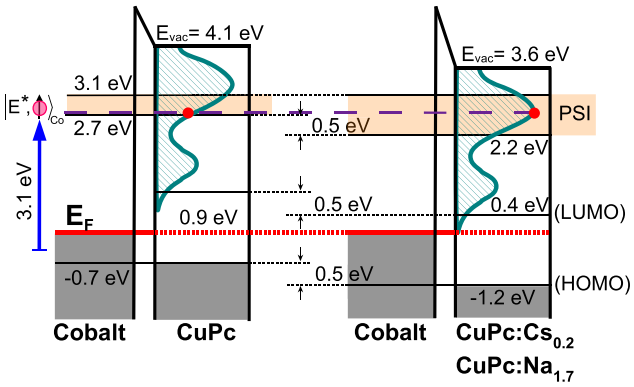

FIG. 2 (color online). Schematic representation of the effect of alkali-metal doping on the electronic properties of CuPc, and relevance for the SR-2PPE measurements. The curves (energy and linewidth) depicting the unoccupied MOs are based upon IPES measurements in [15].

upon doping, electrons with the same energy E^* occupy different electronic states of CuPc, since the MOs are shifted by doping to lower energies, as schematically shown in Fig. 2. The number of photoemitted electrons with spin parallel or antiparallel to the magnetization direction of the cobalt substrate (denoted, respectively, with $N_\uparrow$ and $N_\downarrow$) is detected as a function of E^*. From the values of $N_\uparrow$ and $N_\downarrow$, the spin polarization is calculated according to $P(E^*) = (N_\uparrow - N_\downarrow)/(N_\uparrow + N_\downarrow)$. The spin-injection efficiency F_A is defined as $F_A = P_{\mathrm{CuPc}:A}/P_{\mathrm{Co}}$, where $P_{\mathrm{CuPc}:A}$ is the spin polarization measured from the Co-CuPc:A interface, while P_{Co} is the spin polarization of the bare cobalt surface [13]. By definition, F_A represents the percentage of spin polarization that is preserved after injection from Co into CuPc:A.

Figure 3(a) shows the values of $F_\varnothing$, F_{Cs}, and F_{Na} plotted as a function of the injection energy E^*. Clearly, doping strongly influences the absolute value of the spin-injection efficiency as well as its energy dependence. In particular, $F_\varnothing$ shows a roughly energy-independent behavior, with the average value $\bar{F}_\varnothing = (83 \pm 4)\%$ shown by the black dotted line. On the contrary, the energy dependence of both F_{Na} and F_{Cs} is more pronounced, with a strong maximum at $E^* = 2.7$ eV, where F_{Na} and F_{Cs} assume values above 100%. In order to understand such findings, we have to determine the microscopic scattering mechanisms taking place at the Co-CuPc:A interface, ultimately leading to the observed changes in the spin-dependent population at each energy E^* when the electrons are crossing the interface.

With this aim, we developed a model describing the interface-induced changes in the observables $N_{\uparrow,\downarrow}^{\mathrm{Co}}$ and $N_{\uparrow,\downarrow}^{\mathrm{CuPc}:A}$, respectively defined according to the definition of P_{Co} and $P_{\mathrm{CuPc}:A}$. As schematically depicted in Fig. 3(b), a majority electron excited in the cobalt substrate (belonging to the channel $N_\uparrow^{\mathrm{Co}}$) may undergo the following processes at the Co-CuPc:A interface: (i) Transmission through the interface with energy loss lower than the

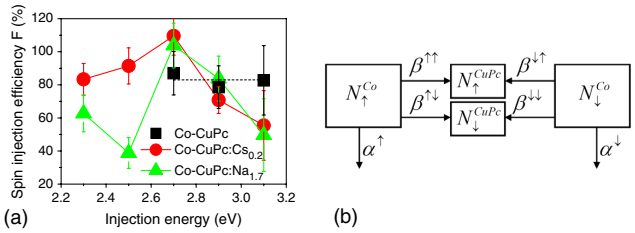

FIG. 3 (color online). (a) Spin-injection efficiency at the Co-CuPc:A interfaces as a function of injection energy; (b) schematic representation of the interface scattering processes considered in our model.

energy resolution set for the experiments ($\Delta E \approx 0.2$ eV) and without spin-flip. After this process, the majority electron will populate the channel $N_\uparrow^{\mathrm{CuPc}:A}$. The quasielastic transmission probability is denoted by $\beta^{\uparrow\uparrow}$. (ii) Transmission through the interface with energy loss lower than ΔE but with a spin-flip. After this process, the majority electron will populate the channel $N_\downarrow^{\mathrm{CuPc}:A}$. The quasielastic spin-flip probability is denoted by $\beta^{\uparrow\downarrow}$. (iii) Reflection or transmission with energy loss higher than ΔE. In both cases, the electron will occupy neither of the channels $N_{\uparrow,\downarrow}^{\mathrm{CuPc}:A}$ at the energy E^*. The loss probability, denoted with $\alpha^\uparrow$, depends on the other two parameters through $\alpha^\uparrow = 1 - (\beta^{\uparrow\uparrow} + \beta^{\uparrow\downarrow})$. The processes relevant for minority electrons (channel $N_\downarrow^{\mathrm{Co}}$) and respective probabilities $\beta^{\downarrow\downarrow}$, $\beta^{\downarrow\uparrow}$, $\alpha^\downarrow$ are shown as well in Fig. 3(b).

If we assume the introduced probabilities to be spin independent, we are left with the following set of two algebraic equations for each energy E^* under consideration:

$$N_{\uparrow,\downarrow}^{\mathrm{CuPc}:A} = \gamma N_{\uparrow,\downarrow}^{\mathrm{Co}} + \beta N_{\downarrow,\uparrow}^{\mathrm{Co}}, \qquad (1)$$

where $\beta \equiv \beta^{\uparrow\downarrow} = \beta^{\downarrow\uparrow}$ is the spin-flip probability, $\gamma \equiv \beta^{\uparrow\uparrow} = \beta^{\downarrow\downarrow}$ the spin-conserving transmission probability, and $\alpha \equiv \alpha^\uparrow = \alpha^\downarrow = 1 - (\beta + \gamma)$ the loss probability. Depending on the values assumed by β we can distinguish between two possible scenarios. If $\beta = 0$, no quasielastic spin-flip processes take place at the interface, and as a consequence, $F_A = 100\%$. On the other hand, for $\beta \neq 0$, quasielastic spin-flip scattering sets in, mixing the spin channels and reducing the value of the spin polarization injected in CuPc:A, thus leading to $F_A < 100\%$.

The probabilities α and β extracted from the experimental data are plotted in Fig. 4 as a function of the injection energy. For $E^* \neq 2.7$ eV, we observe $\beta \neq 0$ for both pristine and doped CuPc, and accordingly, $F_A < 100\%$ [see Fig. 3(a)]. At the same time we have $\alpha \neq 0$, meaning that loss and quasielastic spin-flip scattering events take place simultaneously at the interface independently of doping. A closer look at the data reveals that the probability α has a linear dependency on the injection energy with linear coefficients $K_\varnothing = (0.36 \pm 0.07)\ \mathrm{eV}^{-1}$, $K_{\mathrm{Cs}} = (0.49 \pm 0.04)\ \mathrm{eV}^{-1}$, and $K_{\mathrm{Na}} = (0.56 \pm 0.06)\ \mathrm{eV}^{-1}$. The quasielastic spin-flip probability β shows, on average, higher values after doping. The average values of β (for

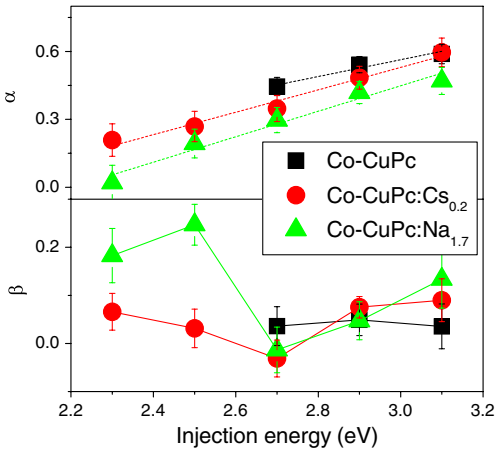

FIG. 4 (color online). Values of the loss probability α and of the quasielastic spin-flip probability β as a function of the injection energy E^*. Linear fits are shown with dotted lines.

$E^* \neq 2.7$ eV) are $\bar{\beta}_{\mathrm{Na}} = 0.15 \pm 0.08$, $\bar{\beta}_{\mathrm{Cs}} = 0.06 \pm 0.02$, and $\bar{\beta}_{\varnothing} = 0.04 \pm 0.01$. The increase of β after doping can be interpreted as an extrinsic effect of doping. It is caused by the alkali-metal atoms at the interface, acting like impurities and thus introducing additional quasielastic spin-flip scattering processes for electrons crossing the interface. For $E^* = 2.5$ eV it holds that $\beta_{\mathrm{Na}} \approx 1.7\overline{\beta}_{\mathrm{Na}}$, and thus a further effect (leading to the pronounced minimum of F_{Na}) cannot be excluded. Assuming $\beta_{\mathrm{Na}} = \beta_{\mathrm{Cs}}$ for $R_{\mathrm{Na}} = R_{\mathrm{Cs}}$, we can extract from our data that the quasielastic scattering probability depends linearly on the dopant concentration with the linear coefficient $0.063 \pm 0.004[\bar{\beta}/R]$. However, one would expect a roughly energy-independent impurity-induced spin-flip scattering probability, which seems to contradict the experimental data.

The reason for the observed strong energy dependency of β will become clear after we discuss the case $E^* = 2.7$ eV. Remarkably, at this injection energy we have $\alpha_{\mathrm{Cs}} \simeq \alpha_{\mathrm{Na}} < \alpha_{\varnothing}$ and $\beta_{\mathrm{Cs}} \simeq \beta_{\mathrm{Na}} \leq 0 < \beta_{\varnothing}$. Correspondingly, the spin-injection efficiency assumes the values $F_{\mathrm{Cs}} = (110 \pm 12)\%$ and $F_{\mathrm{Na}} = (104 \pm 13)\%$, strongly enhanced (up to a factor of 2.7) if compared to the values taken from F_{Cs} and F_{Na} at different energies E^* and also compared to $F_{\varnothing}$. By assuming spin-independent parameters in our model, we obtain $F_A = (\gamma - \beta)/(\gamma + \beta)$, and thus $0 \leq F_A \leq 100\%$. In other words, our assumption implies that the spin polarization of the electrons that crossed the Co-CuPc:A interface ($P_{\mathrm{CuPc}:A}$) cannot be higher than the original spin polarization created in the cobalt substrate (P_{Co}). Values of $P_{\mathrm{CuPc}:A} > P_{\mathrm{Co}}$ can only be obtained with spin-dependent parameters, implying the presence of a MO with majority spin character. Comparing the Perdew-Burke-Erzenhof-hybrid (PBEh) calculations in [20] with the IPES data in [15], we come to the conclusion that in Co-CuPc:$Cs_{0.2}$ and Co-CuPc:$Na_{1.7}$ PBEh predicts a MO (LUMO + 2) at $E^* = 2.7$ eV, in the region where unoccupied MOs are measured with IPES. Because of hybridization or magnetic coupling to the substrate, the (hybrid) interface state at $E^* = 2.7$ eV (originating from such MOs) could possess a majority spin character, resulting in a higher transmission probability for majority electrons and a higher spin-flip probability for minority electrons. This (intrinsic) interface effect is maximum at $E^* = 2.7$ eV, where it overcompensates the detrimental extrinsic doping effect. For $E^* \neq 2.7$ eV the observed energy dependence of the parameter β results from the competition between the two effects.

In summary, we have studied the effect of alkali-metal doping on the spin functionality of a Co-CuPc interface. We can distinguish between an *extrinsic* doping effect, resulting in an increased quasielastic spin-flip scattering probability, and an *intrinsic* effect connected to the doping-induced changes in the interface electronic properties, that can be exploited to actively tailor the spin functionality of the hybrid interface.

Financial support from DFG Research Grant No. AE 19/8-2 is gratefully acknowledged.

*cinchett@rhrk.uni-kl.de

[1] S. Forrest, Nature (London) **428**, 911 (2004).
[2] N. Babescu *et al.*, Nature (London) **327**, 403 (1987).
[3] C. Tang, S. Vanslyke, and C. Chen, J. Appl. Phys. **65**, 3610 (1989).
[4] J. Shi and C. Tang, Appl. Phys. Lett. **70**, 1665 (1997).
[5] J. Kido and T. Matsumoto, Appl. Phys. Lett. **73**, 2866 (1998).
[6] V. Dediu *et al.*, Solid State Commun. **122**, 181 (2002).
[7] Z. Xiong *et al.*, Nature (London) **427**, 821 (2004).
[8] V. Dediu *et al.*, Nature Mater. **8**, 707 (2009).
[9] A. J. Drew *et al.*, Nature Mater. **8**, 109 (2009).
[10] M. Cinchetti *et al.*, Nature Mater. **8**, 115 (2009).
[11] S. Pramanik *et al.*, Nature Nanotech. **2**, 216 (2007).
[12] G. Szulczewki, S. Sanvito, and M. Coey, Nature Mater. **8**, 693 (2009).
[13] O. Andreyev *et al.*, Phys. Rev. B **74**, 195416 (2006).
[14] Y. Gao and L. Yan, Chem. Phys. Lett. **380**, 451 (2003).
[15] H. Ding and Y. Gao, Appl. Phys. Lett. **92**, 053309 (2008).
[16] H. Ding *et al.*, Chem. Phys. Lett. **454**, 229 (2008).
[17] G. Parthasarathy *et al.*, J. Appl. Phys. **89**, 4986 (2001).
[18] H. Ding *et al.*, Phys. Rev. B **78**, 075311 (2008).
[19] For undoped CuPc the PSI was chosen in the range $2.7 \text{ eV} \leq E^* \leq 3.1$ eV in order to exclude every possible detrimental effect from 2PPE transitions with an initial state in CuPc.
[20] N. Maorm *et al.*, J. Chem. Phys. **128**, 164107 (2008).